



Optimization tools for steel portal frames - Effective modelling of lateral supports

Authors: Petr Hradil, Matti Mielonen, Ludovic Fülöp

Confidentiality: Confidential
[Public after closing the project \(July 2010\).](#)

Report's title Optimization tools for steel portal frames – Effective modelling of lateral supports		
Customer, contact person, address Commission of the European Communities		Order reference RFS-PR-06054
Project name Prefabricated steel structures for low-rise buildings in seismic areas		Project number/Short name 12596/PRECASTEEL
Author(s) Petr Hradil, Matti Mielonen, Ludovic Fülöp		Pages 33 p.
Keywords steel, portal frame design, optimization, purlins, lateral stability		Report identification code VTT-R-00566-11
<p>Summary</p> <p>This study brings new insights into the advantages of using more sophisticated design methods for steel portal frames [1] (e.g. geometrically and materially nonlinear analysis with imperfections or GMNIA, and the general method introduced in Eurocode 3 [2]), compared to the commonly used member checks with interaction formulae. The differences between the design alternatives are discussed, focusing on assessing lateral-torsional stability, modelling of lateral supports, and the potential benefits of using advanced shell model instead of widely used beam elements. In addition to the advanced design methods, the topic of shape optimization of frames was explored using real-coded genetic algorithm (GA). The developed optimisation tools highlight the possibility of using GA in everyday design in the future.</p> <p style="text-align: center;">Public after closing the project (July 2010).</p>		
Confidentiality	Confidential	
Espoo 21.1.2011		
Written by	Reviewed by	Accepted by
Petr Hradil Research Scientist	Ludovic Fülöp Senior Research Scientist	Eila Lehmus Technology Manager
VTT's contact address		
Distribution (customer and VTT)		
Customer (Partners of EU-RFCS project PRECSATEEL):		(1 pdf copy each)
VTT/Register Office:		(1 copy)
<p><i>The use of the name of the VTT Technical Research Centre of Finland (VTT) in advertising or publication in part of this report is only permissible with written authorisation from the VTT Technical Research Centre of Finland.</i></p>		

Preface

The results presented in this report were calculated by optimization tools developed in VTT [1] in order to study specific phenomena concerning steel portal frames. Results of different models of lateral supports are included as well as the parametric study of changing snow load.

The material contained in this report is based on the work supported by the European Community's RFS-PR-06054 project PRECASTEEL. This support is gratefully acknowledged. All opinions, findings, conclusions or recommendations expressed in this material are those of the writers. The European Community is not liable for any use of the information contained in this report.

Espoo 21.1.2011

Authors

Contents

Preface	2
1 Introduction.....	4
2 Goal.....	4
3 Description.....	5
3.1 Effect of snow load.....	5
3.2 Effect of lateral supports	5
4 Limitations	6
5 Methods.....	6
5.1 Method 1: Geometrically and materially nonlinear analysis on imperfect structure (GMNIA).....	8
5.2 Method 2: General method	9
5.3 Method 3: EC3 interaction formulae.....	11
5.3.1 In-plane critical amplifier	12
5.3.2 Lateral torsional buckling of eccentrically restrained tapered member	12
5.3.3 Major axis flexural buckling of tapered member.....	12
5.4 Optimization method	13
6 Results	15
6.1 Effect of snow load.....	16
6.2 Effect of lateral supports	19
7 Validation of results	27
8 Conclusions.....	32
9 Summary	32

1 Introduction

Portal frames for industrial buildings have been extensively studied because of their widespread use. The improvement of the design methods for portal frames is one of the recurring topics in the field of steel structures. Due to the large number of similar framed structures, the desire to “automate” the design and manufacturing process was popular from the very early stage [3]. As Dowling et al. [3] noted, there are two design tendencies when trying to achieve more economical solutions: (a) to use compact hot-rolled sections and exploit the advantages of plastic design and (b) to use slender built-up sections with the most advantageous distribution of the material but keep the design in the elastic range. The second option usually leads to slender structures, and therefore stability becomes the main concern of the designer.

In case of side rails and purlins, the elastic design with very slender, Class 4 cross-sections (i.e. cold-formed profiles) tends to be more economical solution compared to the plastically designed hot-rolled continuous purlins. The better distribution of material in cold-formed profiles is clearly offsetting the higher costs of fabrication. Moreover, modern coating technologies also allow the use of material thicknesses in the range of millimetres and below, without fears of corrosion.

Dowling et al. [3] predicted that “an equivalent development towards slender construction in main frame design will lead to similar economies to that achieved with secondary elements”. This conclusion has been supported by the experience in the US [4], Canada and some European countries. However, the situation in Europe is not as clear as in the US where the slender tapered solution almost completely replaced the hot-rolled frames due to the mechanised fabrication of tapered elements. Several European design documents [5], [6], [7], [8] including EN 1993 [1] are more focused on plastic design of frames. In fact, both solutions coexist on the market in many countries.

The economical efficiency of the two solutions depends on several related factors, such as fabrication cost, transport cost, labour cost. Dowling et al. [3] reported weight saving in range of 30% in favour of slender tapered frames. However, it was debated what this means in cost saving [9]. Other aspects of using the welded tapered solutions were also discussed, with important focus on the question of lateral stability of beams and columns [9].

2 Goal

The present study proposes to update the discussion on optimal frame design: (1) by using design methods for stability from the EN 1993 [1], (2) by implementing advanced analysis methods, which are not currently employed by design offices but have potential for replacing current tools, and (3) by introducing optimization tools based on Genetic Algorithms (GA's) to find optimised geometries.

3 Description

3.1 Effect of snow load

The first study based on our optimization tools aims to demonstrate the relation between frame mass (or steel consumption per square meter) and frame span with different snow load and eaves height.

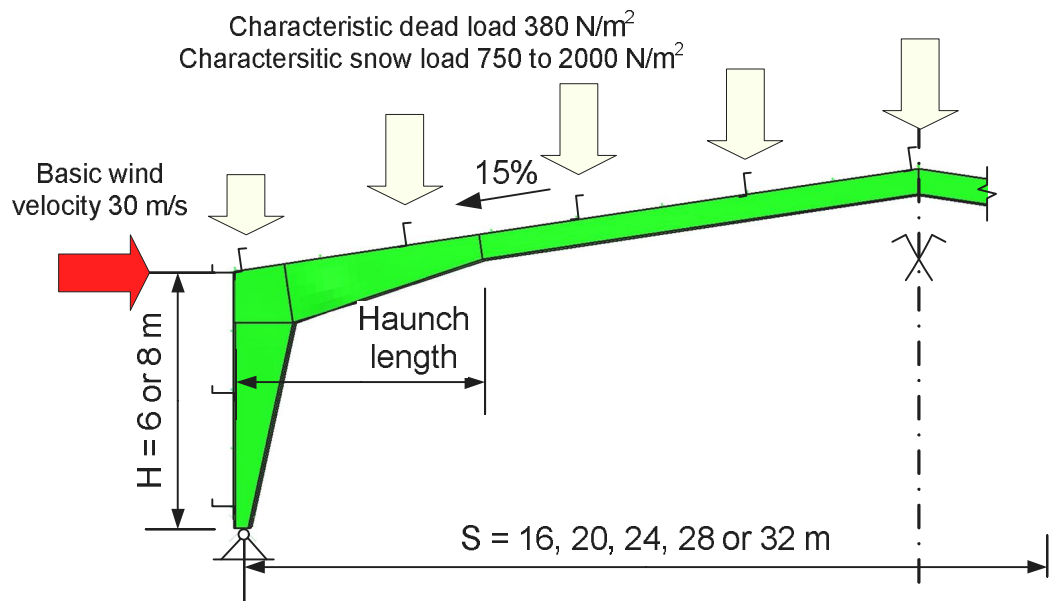


Figure 1 The geometry and loading of the studied welded-tapered frames

Assuming that there is no effective lateral support of compressed flanges, boundary conditions exist only at the external flanges in 3D shell model. The wind load is considered as a secondary variable action creating pressure on upwind side and uplift on downwind side according to EN 1991 [19].

3.2 Effect of lateral supports

The lateral buckling of slender cross-sections is significantly reducing the load-carrying capacity of the frame, and it is common practice to use lateral restraints connected to the inner compressed flanges to suppress this negative effect. The lateral support is usually considered to be strong enough to completely suppress out-of-plane buckling.

However, the most frequently used type of lateral restraint, the diagonal stay, transfers lateral loads by bending of purlins, and tends to be less effective when cold-formed purlins are used. In order to evaluate the behaviour of such frames, the simple 2D beam model is not sufficient. In the following study, 3D model in AP-Frame optimization tool expands by added purlins and lateral restraints.

4 Limitations

The slenderness of frame cross-sections was limited to section class 3 and lower in order to effectively use shell FE models without need of local buckling calculation. Considering class 4 slender cross-sections could save an additional weight, however, very fine mesh needed for the local stability assessment makes the optimization computationally expensive. The steel grade of all calculated cases is S275.

All the optimization results presented in this report were calculated using Genetic Algorithm (GA) method with fixed number of 50 generations and population of 40 individuals in each generation. Although there is no guarantee that the best individual represents the global minimum at the same time, its weight is usually less than 5% higher than the minimal weight.

5 Methods

The study includes several methods for portal frames design to resist loads in fundamental and seismic situations, using the limit states conditions from the EN 1993 [1] and EN 1998 [10]. To implement those design methods in optimization, Abaqus and Excel based plug-ins were developed. Both plug-ins allow automatic generation of computational models and automatic result evaluation. The results of the design checks are expressed as a minimum load amplifier of the design loads to reach the ultimate (ULS) or serviceability (SLS) limit state criteria. The vertical serviceability limit corresponds to an apex deflection of span/200, whereas the horizontal serviceability limit is height/100; derived in a simplified way from EN 1998 [10].

The methods are following the well known scheme described in EN 1993, where the sway imperfections are applied (if needed) to the model prior to calculation of in-plane amplifier which decides about the order analysis. The check for plastic analysis requirements is not implemented (Figure 2) because all of the optimization tools are designed to work mainly with slender frames where elastic analysis should be performed anyway.

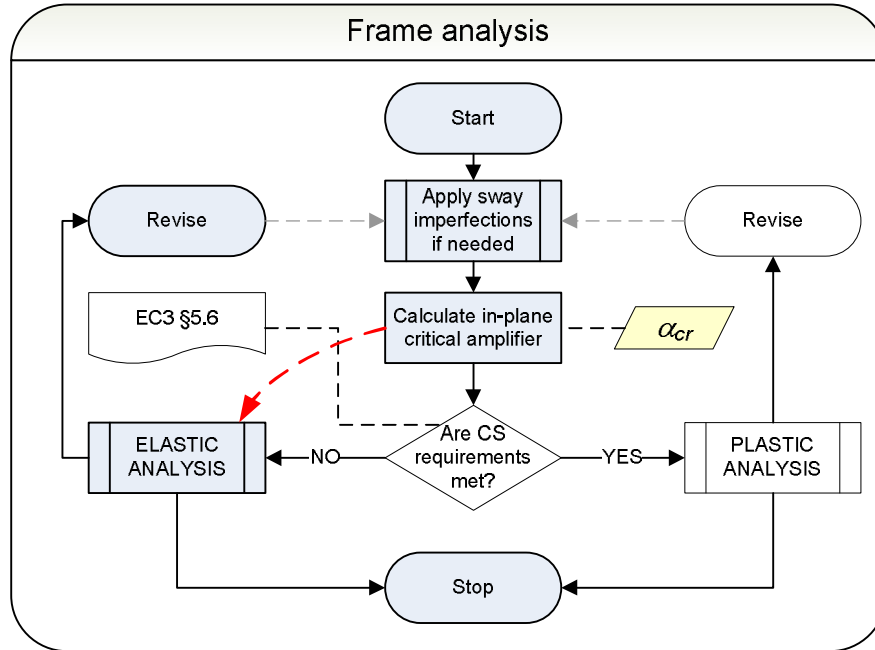


Figure 2 General description of portal frame analysis

The method for sway imperfection accounting is based on modification of model geometry instead of commonly used load amplification (Figure 3). Positions of all nodes are shifted horizontally in order to achieve calculated global initial sway imperfection at eaves height in 2D and 3D models. There is no check whether sway imperfections could be neglected in the optimization tools, and they are applied automatically to each model.

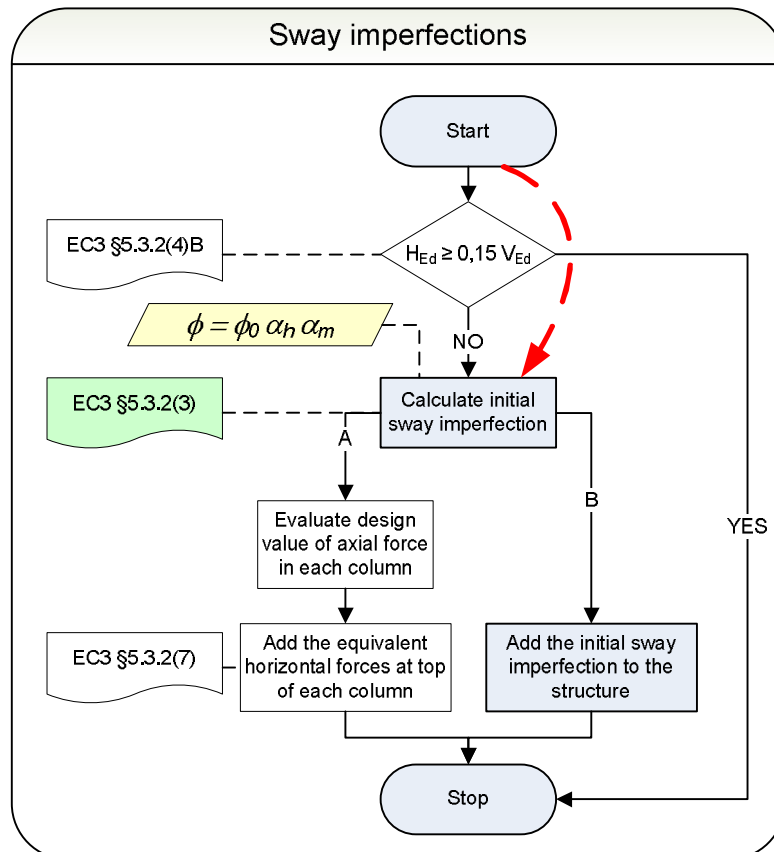


Figure 3 General rules for applying sway imperfections

5.1 Method 1: Geometrically and materially nonlinear analysis on imperfect structure (GMNIA)

The most computationally expensive method is the straightforward numerical calculation of 3D shell model of the frame. No special checks for out-of-plane stability are needed in such method, because the calculation is materially and geometrically nonlinear and is taking into account appropriate initial bow imperfections.

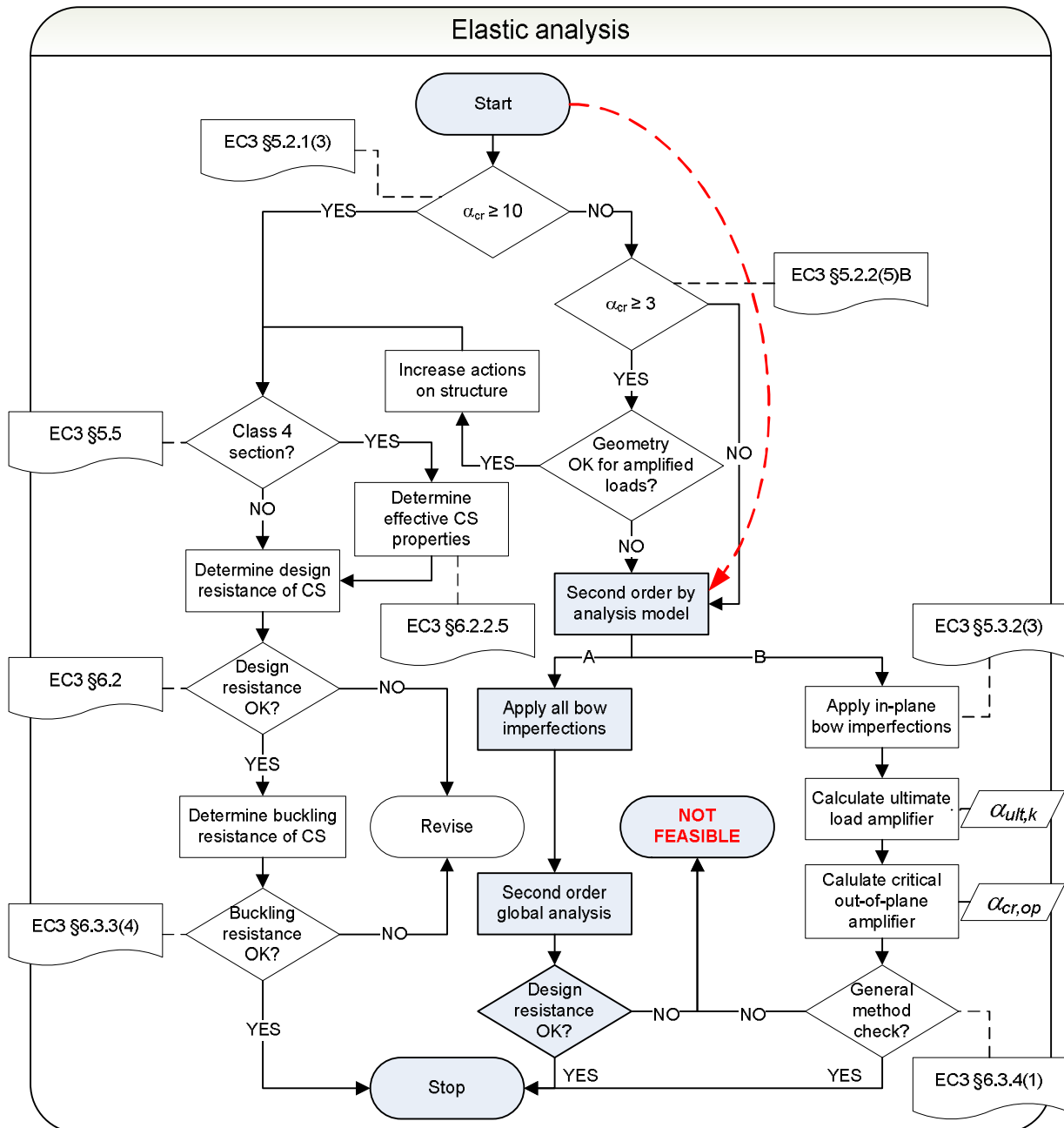


Figure 4 Second order elastic analysis with Method 1 (GMNIA)

GMNIA is already the second-order analysis and therefore no further checks of in-plane critical amplifier are needed. Imperfections are inserted from a preliminary eigenvalue analysis, using the first positive buckling shape of the model, scaled to the EN 1993 [1] recommended amplitude (i.e. using Table 5.1 from EN 1993).

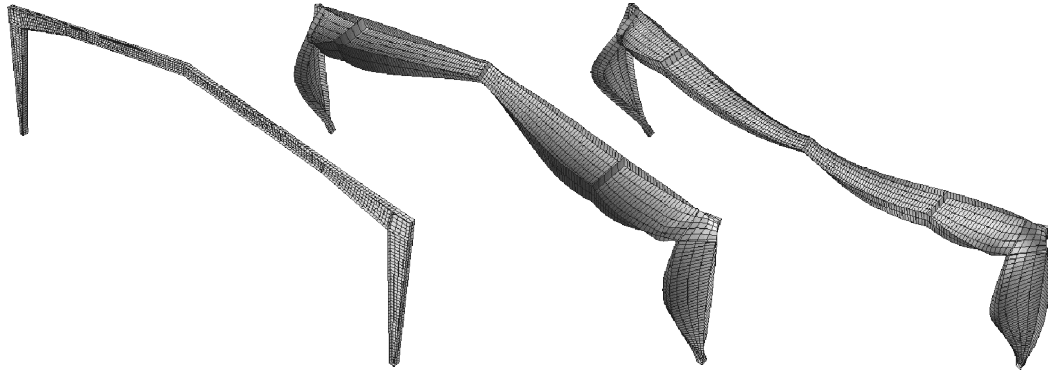


Figure 5 Global nonlinear analysis calculation steps: Undeformed model (left), First buckling shape (middle), Deformation during nonlinear analysis with increasing vertical loads (right - scale: 20)

5.2 Method 2: General method

This method takes into account out-of-plane stability with a global reduction factor. Because of the particularly difficult analytical expression of critical load of frames which are made from eccentrically supported members with variable cross-sections, the method is using 3D shell model for the evaluation of the critical amplifier.

According to EN 1993 [1], the resistance of the frame is checked using the following condition:

$$\frac{\chi_{op} \cdot \alpha_{ult,k}}{\gamma_{M1}} \geq 1,0 \quad (1)$$

where $\alpha_{ult,k}$ is the minimum load amplifier of the design loads to reach the characteristic resistance of the most critical cross-section without out-of-plane buckling effect. This value is the result of a nonlinear analysis with gradually increasing loads on a 2D beam model with in-plane bow and sway imperfections. Out-of-plane buckling reduction factor χ_{op} originates from the critical amplifier $\alpha_{cr,op}$ of the design loads to reach the elastic critical resistance with regards to lateral or lateral torsional buckling.

Method 2 has the advantage of faster numerical calculation compared to Method 1. The computational advantage results from the use of the simplified 2D beam model for the nonlinear part of the analysis.

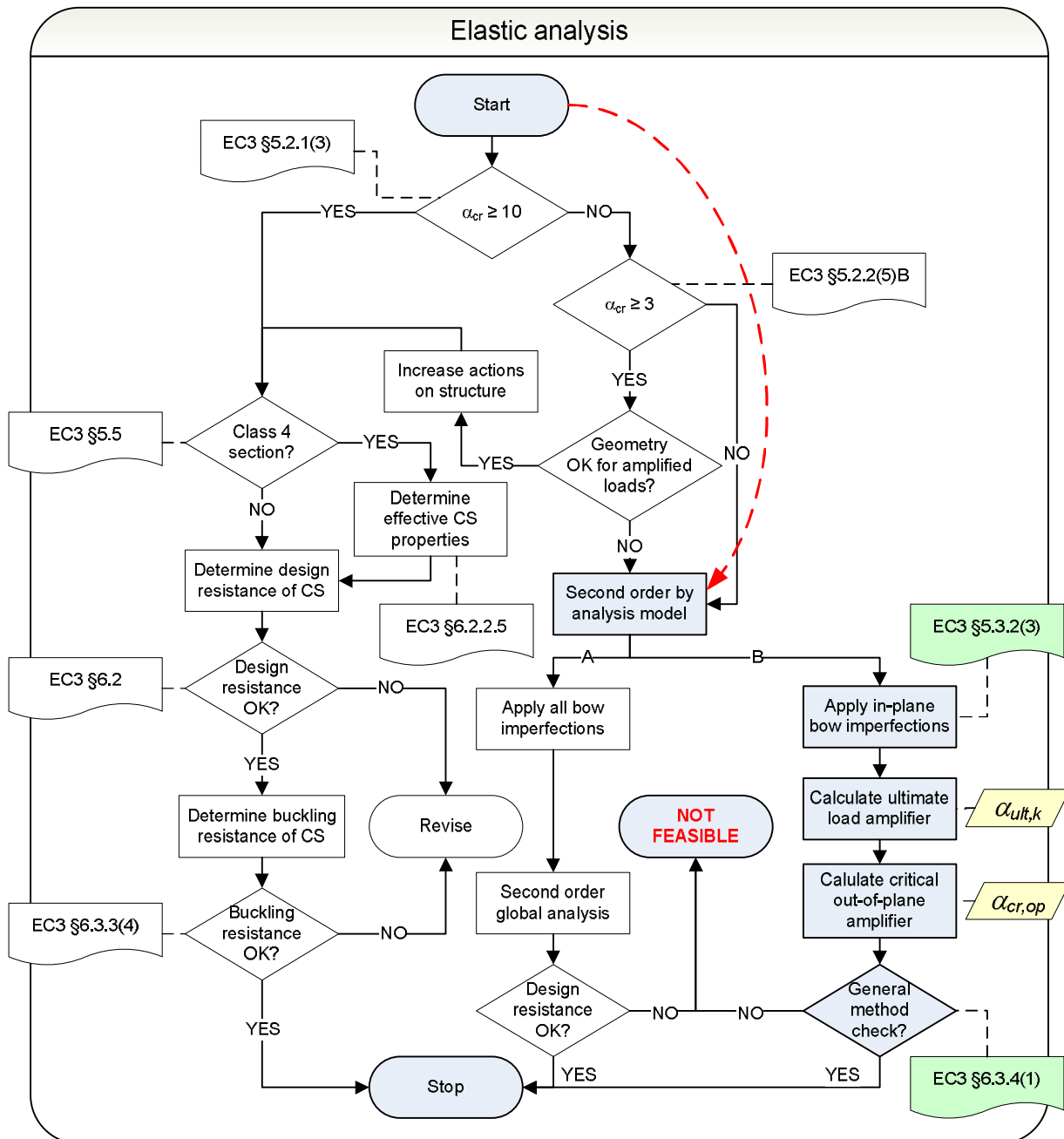


Figure 6 Second order elastic analysis with Method 2 (General Method)

The Method 3 uses the following modifications of the calculation described in EN 1993 [1]:

5.3.1 In-plane critical amplifier

While the critical load was a result of linear eigenvalue analysis in Method 2, the analytical approach is adapted in this case. The calculations take into account the presence of the axial force in the rafters and utilize the formulas proposed by Davies [11].

5.3.2 Lateral torsional buckling of eccentrically restrained tapered member

The critical moment in our calculation is the smaller value of critical moment of restrained member between fork supports according to SCI Technical Report [8] and critical moment of unrestrained part of member between purlins or side rails according to EN 1993 [1]:

$$M_{cr} = \min \left[\left(\frac{1}{m_t c^2} \right) M_{cr0}, C_1 \frac{\pi^2 E \cdot I_{z,\min}}{a^2} \sqrt{\frac{I_{w,\min}}{I_{z,\min}} + \frac{a^2 G \cdot I_{t,\min}}{\pi^2 E \cdot I_{z,\min}}} \right] \quad (2)$$

$$M_{cr0} = \left(\frac{i_0^2}{2e_z} \right) N_{cr,TFB} \quad (3)$$

Here m_t is equivalent uniform moment factor adapted from [7], $I_{y,\min}$, $I_{z,\min}$, and $I_{w,\min}$ are sectional properties of the shallow end, a is the distance between lateral supports (purlins, side rails), $N_{cr,TFB}$ stands for critical axial load of torsional flexural buckling of eccentrically restrained member, C_1 is the moment gradient factor from EN 1993 [1], e_z is the distance from shear centre to lateral support either at shallow end or at deep end of tapered beam.

When the relative slenderness is higher than 1, equivalent section factor c is also 1 and the minimum $M_{cr,0}$ was used, which comes from the deepest end. In all other cases shallow end properties and following expression for equivalent section factor are used:

$$c = 1 + (c_0 - 1) \sqrt{L_h / L} \quad (4)$$

where L_h and L are the lengths of haunch and the whole member respectively and the basic equivalent section factor c_0 was adapted from [8].

5.3.3 Major axis flexural buckling of tapered member

It is very conservative to apply the standard formula for calculation of the critical load of the tapered member using the shallow end's sectional properties. A more accurate option is the approach proposed by Šapalas [12] used in Method 3, where critical loads are based on the deep end cross-sectional properties and reduced by α_n factor.

5.4 Optimization method

The portal frame optimization problem is both nonlinear and discrete, which causes difficulties for classical direct and gradient-based optimization methods. On the other hand, genetic algorithms (GAs) are successfully applied in the field of structural optimization [13], [14], [15] and [16]. GAs have several advantages, such as possibility of parallel computing, easy handling of multiple variables, and straightforward coding practice. Genetic algorithm is a procedure which tries to mimic the natural evolution process. After an initial population is created and analysed, the fitness of each individual is evaluated. Then a new population is created by favouring the fittest individuals and by combining the properties of the population members using genetic operators, such as crossover and mutation. GA proceeds iteratively towards the optimal solution by creating a new population using the properties of the previous one. Elitism ensures that the best solution is kept during all of the genetic operations, and while no proof of convergence in finite time exists, good results are found in a reasonable time.

A real-coded genetic algorithm (RCGA) can handle discrete and real variable types easily and has been chosen for this problem. With RCGA, the coding-decoding characterizing binary-coded GAs is also avoided.

Optimization literature provides a large catalogue of different selection, crossover and mutation operators that can be combined to create a GA suited for the problem at hand. In this report, the well known simulated binary crossover (SBX) [17] and parameter based polynomial mutation operator [13] are utilized. The crossover operator has a self-adapting behaviour, which favours creating children near to parents, when the parents are near to each other in the variable space. The basic behaviour of the genetic algorithm is enhanced by two methods developed to improve the steel portal frame optimization:

- a local search method is creating individuals very similar to the current elite individual found, which ensures that the local optimum is found with very high probability;
- the diversity of the population is maintained by using so called diversifying operator, which introduces new genetic material to the population preventing premature convergence to the local optimum [16].

In terms of optimization objective function, it has been opted to concentrate on easily measurable performance parameters, such as weight, with the flexibility to expand results to more financially oriented targets (e.g. price).

The algorithm can be used with all of the design methods and the flowchart of the optimization combined with design methods is presented in Figure 8.

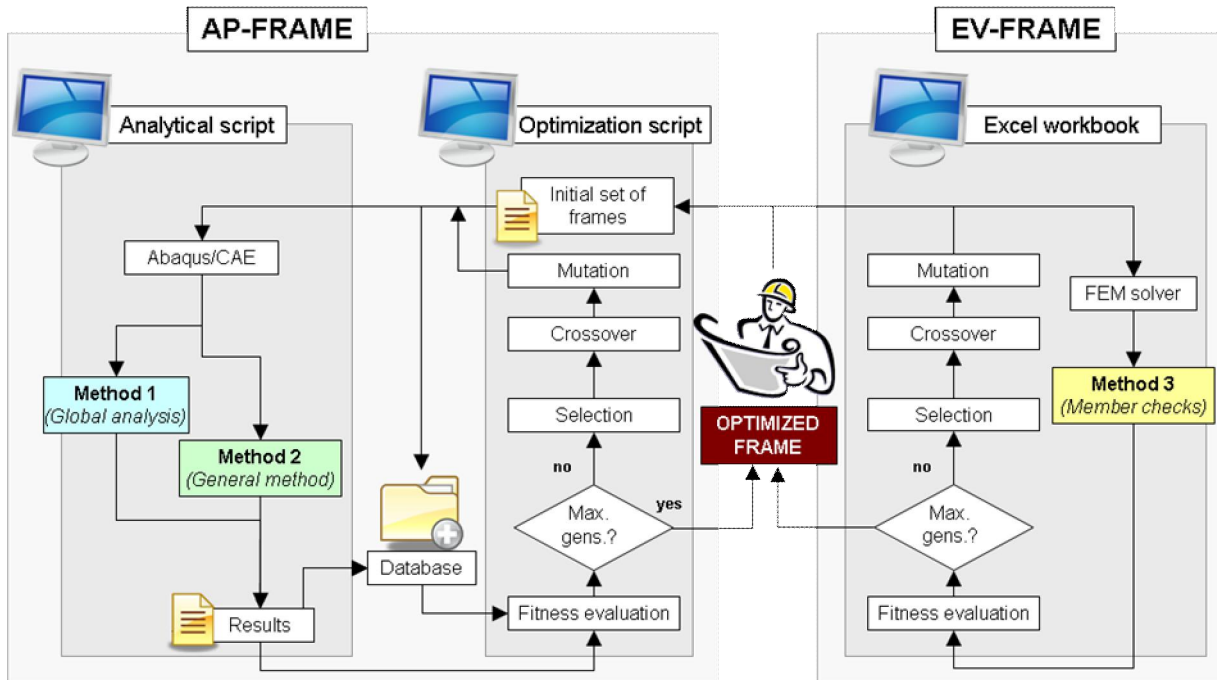


Figure 8 The basic diagram of two optimization tools developed at VTT

AP-Frame contains the Abaqus based design methods and optimization, whereas EV-Frame refers to the design and optimization developed in a Microsoft Excel workbook. In both cases, the GA runs for predetermined number of generations, and the best configuration found is given as an output. Figure 9 presents five example optimisation runs of the same frame configuration, which shows how the weight of the elite individual typically decreases during the genetic algorithm optimisation. In this example, eight variables were optimized in a welded-tapered frame with population size 20 and maximum 50 generations.

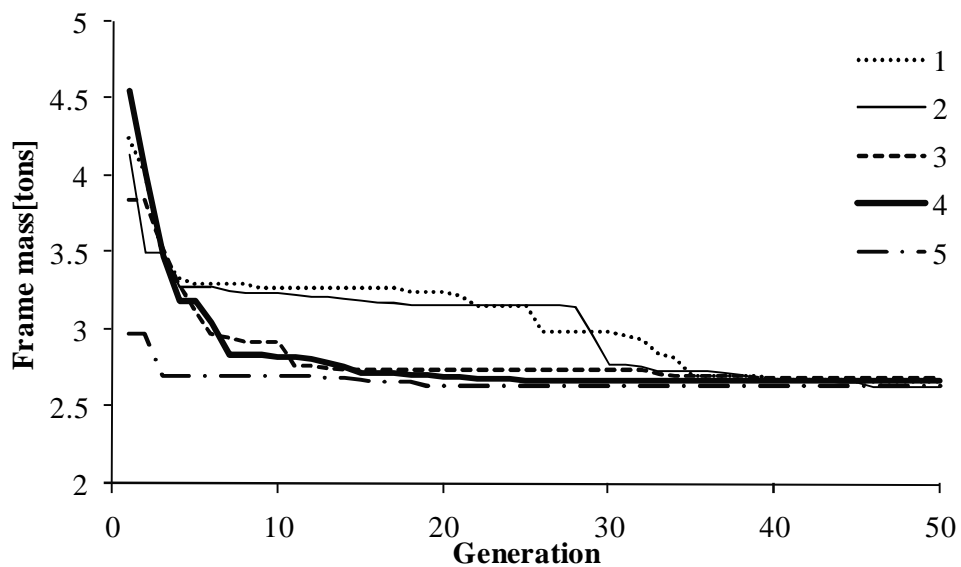


Figure 9 Elite value fitness development in five optimisations of the same frame configuration with the genetic algorithm.

Typically, the weight of the elite frame in the population decreases sharply during the first generations, and then the search focuses around the elite individual

refining the solution. Sudden drop in fitness occurs usually when the algorithm finds a better alternative typology, meaning that many variables can change drastically.

6 Results

The most important feature of the optimization tools is the ability to find the lowest mass of welded-tapered frames where millions of combinations are possible because of multiple variable parameters. Besides cross-section geometry, there are usually several other variables such as roof angle and the length of the haunch. In our study, we used fixed roof pitch of 15% and variable haunch length.

The unique names of column and rafter are composed of their dimensions in mm (Figure 10). For example column 200x800x260x12x6 means that tapered section's shallow end is 200 mm high while the deep end is 800 mm high, flanges are 260x12 mm and web thickness is 6 mm. Also the length of the haunch (Lh) has to be provided as the rafter is tapered only at the frame corner. Sometimes the length is expressed as the haunch ratio (S/Lh).

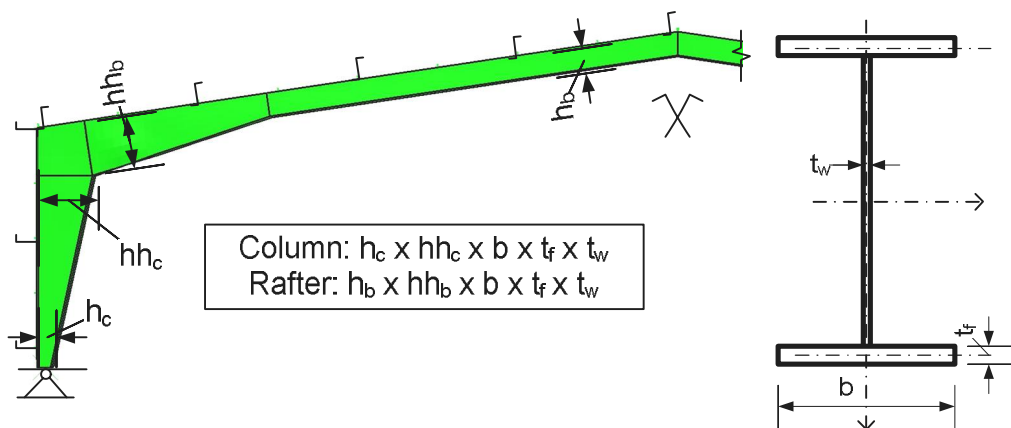


Figure 10 Column and rafter names

6.1 Effect of snow load

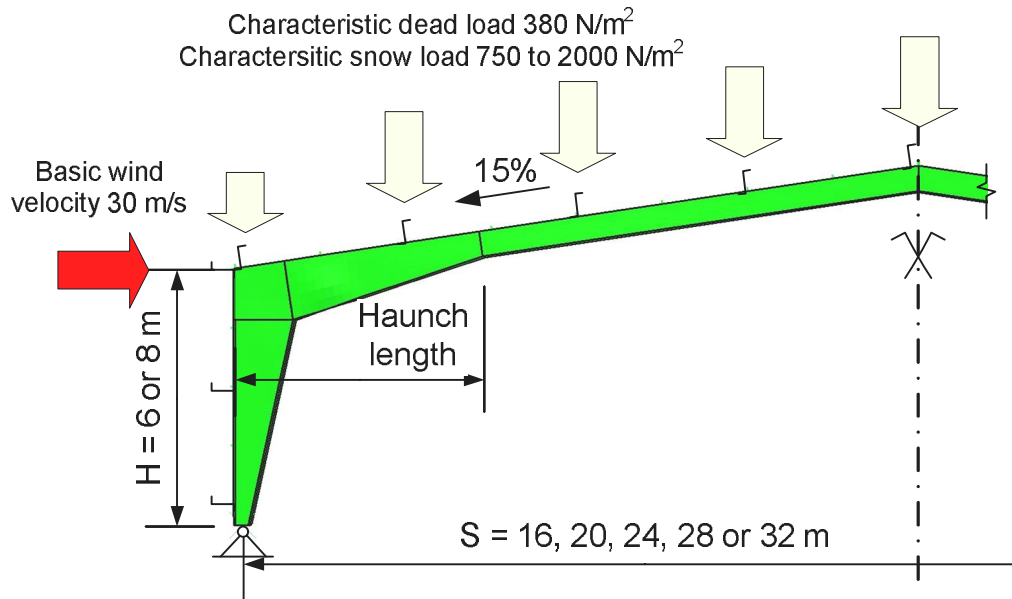


Figure 11 The geometry and loading of the studied welded-tapered frames

The first study based on our optimization tools aims to demonstrate the relation between frame mass (or steel consumption per square meter) and frame span (Figure 12) with different snow load and eaves height. Assuming that there is no effective lateral support of compressed flanges, boundary conditions exist only at the external flanges in 3D shell model. Also the wind load is considered as a secondary variable action creating pressure on upwind side and uplift on downwind side according to EN 1991 [19] (Figure 11).

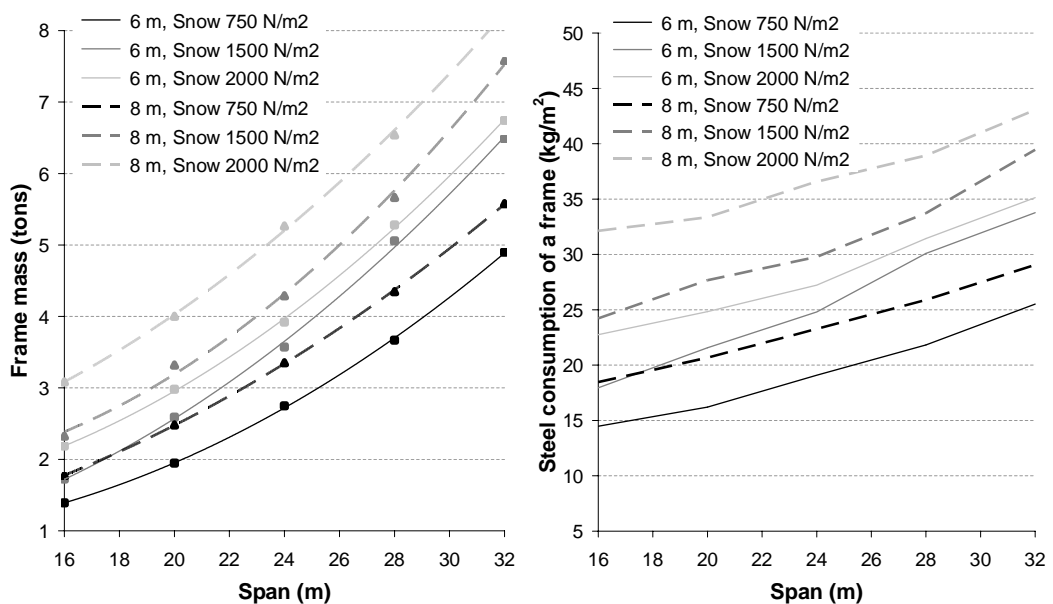


Figure 12 The effect of different snow loads on welded-tapered frames 6 m high (solid line) and 8 m high (dashed). The load is represented as a characteristic value on flat roof (e.g. 2000 N/m² corresponds to basic snow load 2500 N/m² on the ground)

Table 1 Optimization of 6 m high welded-tapered frames with different snow load

(a) Optimization of 6 m high frames with 750 N/m ² characteristic snow load calculated with AP-Frame General Method (Method 2) with no lateral supports on the inner flanges					
Span (m)	Column	Rafter	Haunch ratio (S/L _h)	Frame mass (tons)	Steel consumption (kg/m ²)
16	220x560x220x10x5	360x560x220x10x5	7	1.390	14.5
20	260x640x260x10x6	380x640x260x10x6	8	1.946	16.2
24	300x600x300x12x6	380x600x300x12x6	8	2.749	19.1
28	320x640x320x14x6	420x640x320x14x6	9	3.667	21.8
32	340x820x340x14x8	560x820x340x14x8	10	4.899	25.5
(b) Optimization of 6 m high frames with 1500 N/m ² characteristic snow load calculated with AP-Frame General Method (Method 2) with no lateral supports on the inner flanges					
Span (m)	Column	Rafter	Haunch ratio (S/L _h)	Frame mass (tons)	Steel consumption (kg/m ²)
16	260x660x260x10x6	400x660x260x10x6	9	1.724	18.0
20	320x640x320x12x6	380x640x320x12x6	9	2.589	21.6
24	340x680x340x14x6	500x680x340x14x6	10	3.571	24.8
28	380x860x380x15x8	540x860x380x15x8	10	5.056	30.1
32	400x800x400x18x8	500x800x400x18x8	10	6.485	33.8
(c1) Optimization of 6 m high frames with 2000 N/m ² characteristic snow load calculated with EV-Frame (Method 3) with no lateral supports on the inner flanges					
Span (m)	Column	Rafter	Haunch ratio (S/L _h)	Frame mass (tons)	Steel consumption (kg/m ²)
16	360x560x300x12x5	440x560x300x12x5	11	2.152	22.4
20	400x900x300x12x8	400x900x300x12x8	6	2.948	24.6
24	400x1120x300x12x10	460x1120x300x12x10	5	3.885	27.0
28	380x900x380x15x8	560x900x380x15x8	9	5.220	31.1
32	440x1120x400x15x10	520x1120x400x15x10	5	6.680	34.8
(c2) Optimization of 6 m high frames with 2000 N/m ² characteristic snow load calculated with AP-Frame GMNIA (Method 1) with no lateral supports on the inner flanges					
Span (m)	Column	Rafter	Haunch ratio (S/L _h)	Frame mass (tons)	Steel consumption (kg/m ²)
16	260x660x260x10x8	460x660x260x10x8	11	1.971	20.5
20	280x880x280x12x8	420x880x280x12x8	6	2.732	22.8
24	300x900x300x15x8	580x900x300x15x8	11	3.889	27.0
28	340x1080x340x14x10	600x1080x340x14x10	8	5.092	30.3
32	380x1100x380x15x10	700x1100x380x15x10	11	6.482	33.8

Table 2 Optimization of 8 m high welded-tapered frames with different snow load

(d) Optimization of 8 m high frames with 750 N/m ² characteristic snow load calculated with AP-Frame General Method (Method 2) with no lateral supports on the inner flanges					
Span (m)	Column	Rafter	Haunch ratio (S/L _h)	Frame mass (tons)	Steel consumption (kg/m ²)
16	240x560x240x10x5	500x560x240x10x5	10	1.773	18.5
20	240x680x240x12x6	540x680x240x12x6	10	2.481	20.7
24	320x620x320x12x6	500x620x320x12x6	10	3.352	23.3
28	340x640x340x14x6	500x640x340x14x6	10	4.348	25.9
32	360x840x360x14x8	560x840x360x14x8	10	5.578	29.1
(e) Optimization of 8 m high frames with 1500 N/m ² characteristic snow load calculated with AP-Frame General Method (Method 2) with no lateral supports on the inner flanges					
Span (m)	Column	Rafter	Haunch ratio (S/L _h)	Frame mass (tons)	Steel consumption (kg/m ²)
16	280x620x280x12x6	380x620x280x12x6	9	2.325	24.2
20	320x680x320x14x6	420x680x320x14x6	10	3.320	27.7
24	360x640x360x15x6	440x640x360x15x6	11	4.289	29.8
28	400x800x400x15x8	480x800x400x15x8	8	5.665	33.7
32	380x920x380x20x8	580x920x380x20x8	9	7.576	39.5
(f1) Optimization of 8 m high frames with 2000 N/m ² characteristic snow load calculated with EV-Frame (Method 3) with no lateral supports on the inner flanges					
Span (m)	Column	Rafter	Haunch ratio (S/L _h)	Frame mass (tons)	Steel consumption (kg/m ²)
16	480x560x320x14x5	540x560x320x14x5	10	3.033	31.6
20	400x680x360x14x6	600x680x360x14x6	11	3.946	32.9
24	540x680x400x15x6	680x680x400x15x6	9	5.185	36.0
28	460x1120x380x15x10	600x1120x380x15x10	8	6.474	38.5
32	460x880x440x18x8	640x880x440x18x8	11	8.167	42.5
(f2) Optimization of 8 m high frames with 2000 N/m ² characteristic snow load calculated with AP-Frame GMNIA (Method 1) with no lateral supports on the inner flanges					
Span (m)	Column	Rafter	Haunch ratio (S/L _h)	Frame mass (tons)	Steel consumption (kg/m ²)
16	260x840x260x10x8	500x840x260x10x8	8	2.395	24.9
20	320x820x320x12x8	440x820x320x12x8	7	3.356	28.0
24	320x1060x320x12x10	640x1060x320x12x10	8	4.573	31.8
28	360x1060x360x14x10	640x1060x360x14x10	8	5.883	35.0
32	400x1120x400x15x10	820x1120x400x15x10	11	7.611	39.6

6.2 Effect of lateral support models

The lateral buckling of slender cross-sections is significantly reducing the load-carrying capacity of the frame, and it is common practice to use lateral restraints connected to the inner compressed flanges to suppress this negative effect. The lateral support is usually considered to be strong enough to completely suppress out-of-plane buckling.

However, the most frequently used type of lateral restraint, the diagonal stay, transfers lateral loads by bending of purlins, and tends to be less effective when cold-formed purlins are used. In order to evaluate the behaviour of such frames, the simple 2D beam model is not sufficient. In the following study, 3D model in AP-Frame optimization tool expands by added purlins and lateral restraints (Figure 13). The purlins are modelled as beam elements with 2 mm thick Z150 cross-section, and lateral stays are simplified as rigid truss elements. The diagonal stays exist only in the corner region of the frame supporting the whole length of the haunch and one third of the column. It has been tested that adding more supports has no further effect on lateral stability of the frame.

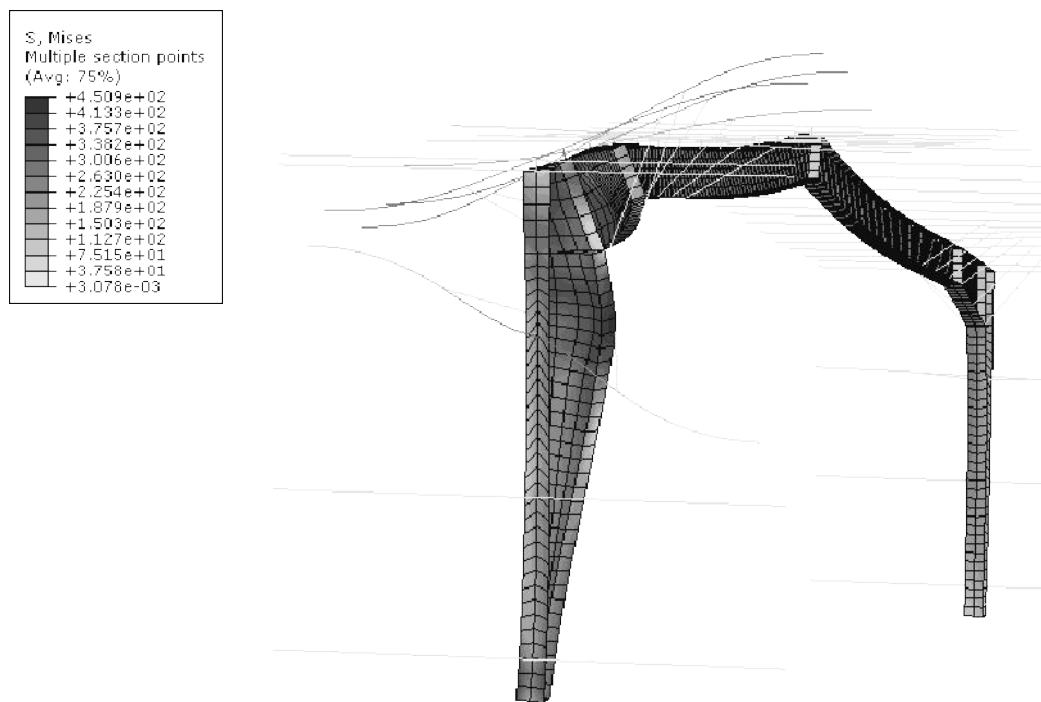


Figure 13 The lateral torsional buckling failure of 6 m high frame with 32 m span (5x scaled) considering support of purlins.

The calculation covers 6 m high frames with basic snow load 2500 N/m^2 and basic wind velocity 30 m/s according to EN 1991 [19]. The weight of welded-tapered frames without any supports as well as fully restrained frames (Figure 14) is optimized for comparison. As it can be observed, the lateral supports in smaller frames restrains the out-of-plane buckling very well while the effect of those supports rapidly decreases with increasing span. This indicates that light gauge steel purlins can be relied upon for stabilizing smaller span frames, but they are not effective when the span increases.

The graphs can also give an indication to the designer whether providing diagonal stays is economical. Implementing diagonal stays in the design of structure brings an extra expense: it requires connecting plates to be welded on the main frame and it very often disrupts the internal sheeting. The gain in terms of material consumption on the frame might not offset the expenses. In any case, the lateral stabilization of the frame has to be modelled using 3D model with proper support stiffness to correctly account for their effect.

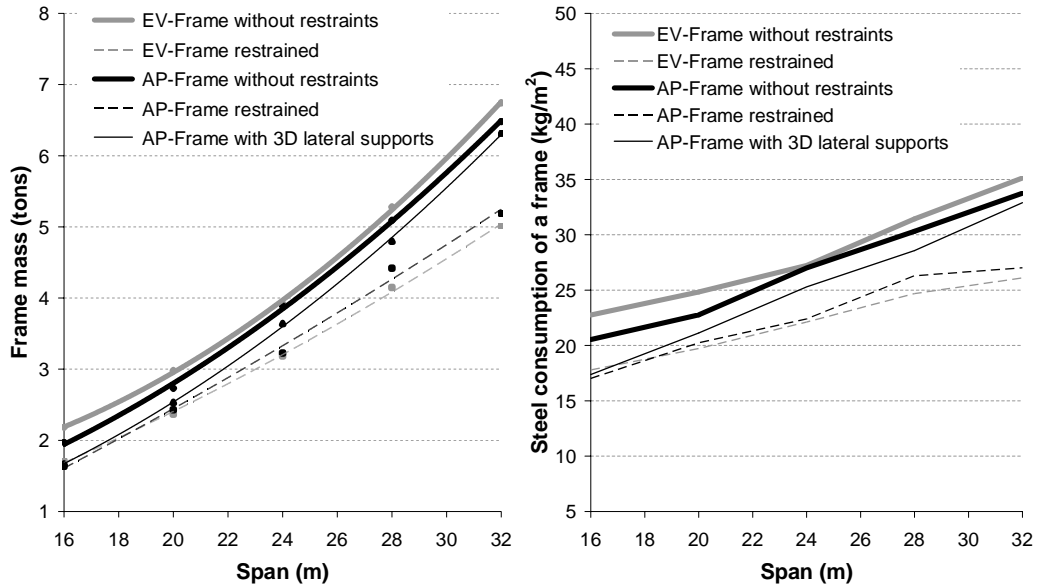


Figure 14 The effect of out-of-plane buckling studied on 6 m high welded-tapered frames with purlins and diagonal stays included in the model (solid fat line) compared to models without any lateral restraints (solid thin line) and fully restrained (dashed line) using different design methods.

Table 3 Optimization of 6 m high welded-tapered frames with different lateral restraints

(a) Optimization of 6 m high frames with 2000 N/m ² characteristic snow load calculated with EV-Frame (Method 3) with no lateral supports on the inner flanges - see Table 1 (c1) -					
(b) Optimization of 6 m high frames with 2000 N/m ² characteristic snow load calculated with EV-Frame (Method 3) with full lateral support					
Span (m)	Column	Rafter	Haunch ratio (S/L _h)	Frame mass (tons)	Steel consumption (kg/m ²)
16	260x680x220x10x6	560x680x220x10x6	11	1.687	17.6
20	320x900x200x12x8	500x900x200x12x8	10	2.345	19.5
24	240x900x240x14x8	500x900x240x14x8	10	3.156	21.9
28	520x1120x260x10x10	740x1120x260x10x10	10	4.111	24.5
32	400x1100x320x12x10	540x1100x320x12x10	6	4.972	25.9
(c) Optimization of 6 m high frames with 2000 N/m ² characteristic snow load calculated with AP-Frame GMNIA (Method 1) with no lateral supports on the inner flanges - see Table 1 (c2) -					
(d) Optimization of 6 m high frames with 2000 N/m ² characteristic snow load calculated with AP-Frame GMNIA (Method 1) with full lateral support					
Span (m)	Column	Rafter	Haunch ratio (S/L _h)	Frame mass (tons)	Steel consumption (kg/m ²)
16	120x900x120x14x8	520x900x120x14x8	8	1.634	17.0
20	240x880x240x10x8	620x880x240x10x8	8	2.430	20.2
24	260x1100x260x10x10	500x1100x260x10x10	6	3.226	22.4
28	280x1120x280x12x10	720x1120x280x12x10	10	4.417	26.3
32	280x1320x280x12x12	500x1320x280x12x12	5	5.188	27.0
(e) Optimization of 6 m high frames with 2000 N/m ² characteristic snow load calculated with AP-Frame GMNIA (Method 1) with semi-rigid lateral supports on the inner flanges					
Span (m)	Column	Rafter	Haunch ratio (S/L _h)	Frame mass (tons)	Steel consumption (kg/m ²)
16	200x880x200x8x8	520x880x200x8x8	8	1.668	17.4
20	220x900x220x12x8	620x900x220x12x8	10	2.534	21.1
24	260x1020x260x12x10	640x1020x260x12x10	9	3.626	25.2
28	300x1100x300x15x10	540x1100x300x15x10	7	4.801	28.6
32	320x1100x320x18x10	640x1100x320x18x10	9	6.317	32.9

6.3 Effect of lateral support positions

The optimal position of lateral diagonal braces was investigated in a short study on welded-tapered frame with 24 m span, 6 m eaves height and 6 m centres distance. Two frames with equally distributed supports (Case 1 - Figure 15 and Case 2 - Figure 17) and two frames with supports concentrated at the corner (Case 3 - Figure 19, Case 4 - Figure 21 and Case 5) were compared with the unrestrained frame (Case 0). In each configuration two frames were calculated with different column supports. For columns, the diagonal braces were placed near the frame corner all the time.

The frames were calculated with AP-Frame tool using GMNIA (Method 1) and 3D shell model of frame extended with wire model of purlins and lateral braces.

In the following table (Table 4) several load amplifiers were extracted from the calculation reports. α_{cr} is the first positive critical amplifier from the linear buckling calculation, $\alpha_{ult,el}$ is the amplifier of the design vertical load to reach the elastic load (where the yield stress is reached) in the non-linear analysis on imperfect structure and $\alpha_{ult,max}$ is the maximum load amplifier from the same analysis.

Table 4 Load amplifiers of welded-tapered frames with different lateral support positions

Case	Rafter supports	Column supports	α_{cr}	$\alpha_{ult,el}$	$\alpha_{ult,max}$
0	-----	----	2.7553	1.47369	1.71767
1a	X--X--X	----	3.3647	1.47653	1.81521
1b	X--X--X	-X--	4.0127	1.72327	2.19378
2a	X-X-X-X	----	3.7529	1.5387	1.88835
2b	X-X-X-X	-X--	4.4074	1.74484	2.25836
3a	XX-----	-X--	4.3942	1.8311	2.35169
3b	XX-----	-XX-	4.8239	1.87449	2.56356
4a	XXX-----	-X--	4.7571	1.76147	2.31624
4b	XXX-----	-XX-	5.7633	1.71541	2.3861
5a	XXXX----	-X--	4.7625	1.76238	2.3184
5b	XXXX----	-XX-	5.7692	1.71505	2.37921

Note that the most efficient configuration is 3b with two supports on the rafter and two supports on the column. However, the lowest cost could be achieved in another case (e.g. 3a) with smaller material consumption and smaller number of structural joints.

The first two studies (Case 1 and Case 2) show the importance of at least one column support that is able to increase the ultimate capacity by 20% in both cases. Adding another column support (Case 3 and Case 4) has only minor effect for this particular frame.

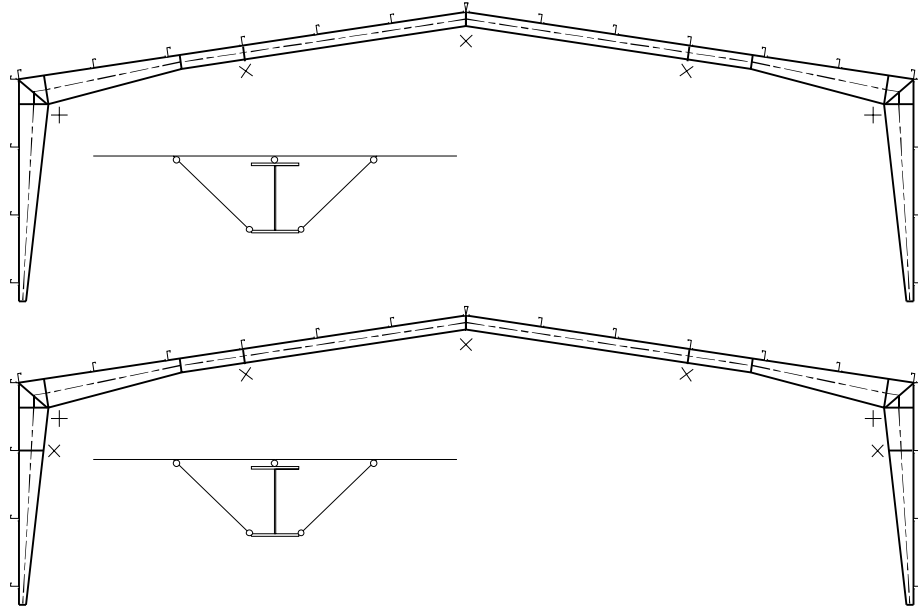


Figure 15 Case 1 supported every 3rd purlin a) without column supports b) with one column support 4,2 m above the ground

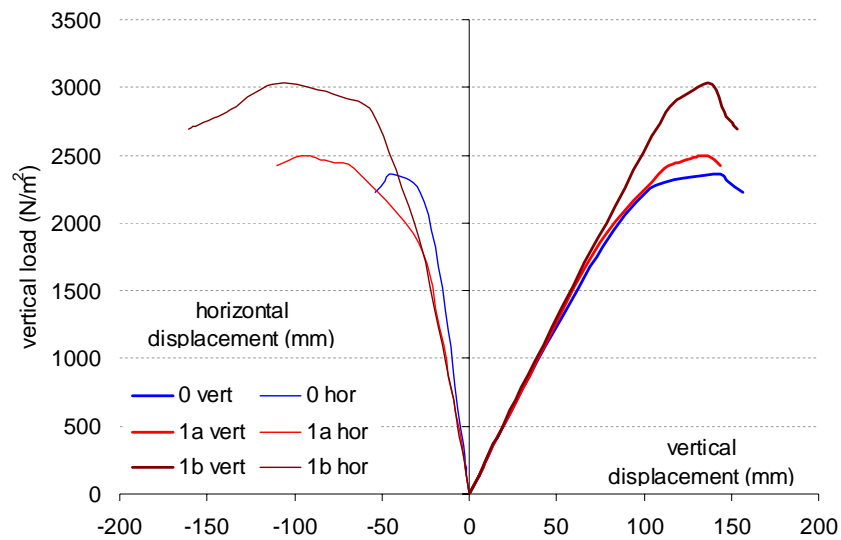


Figure 16 Load-displacement relationship (horizontal left, vertical right) of the restrained (Case 1) and unrestrained (Case 0) frames

Another interesting effect which could be observed in all studied frames is the small increase of vertical stiffness and small decrease of horizontal stiffness when the supports are applied. The latter one could be critical for horizontal serviceability checks in some cases, especially in pinned frames in seismic areas.

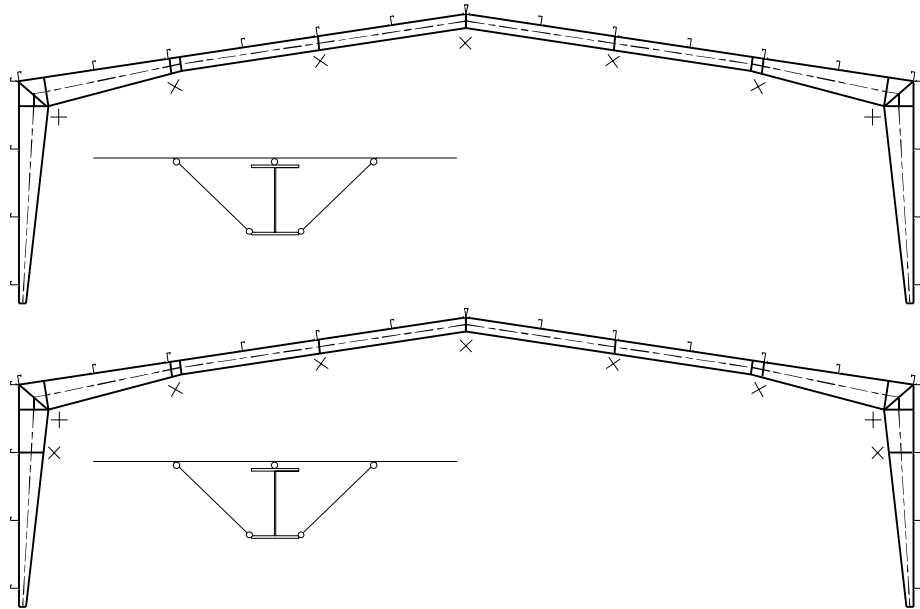


Figure 17 Case 2 supported every 2nd purlin a) without column supports b) with one column support 4,2 m above the ground

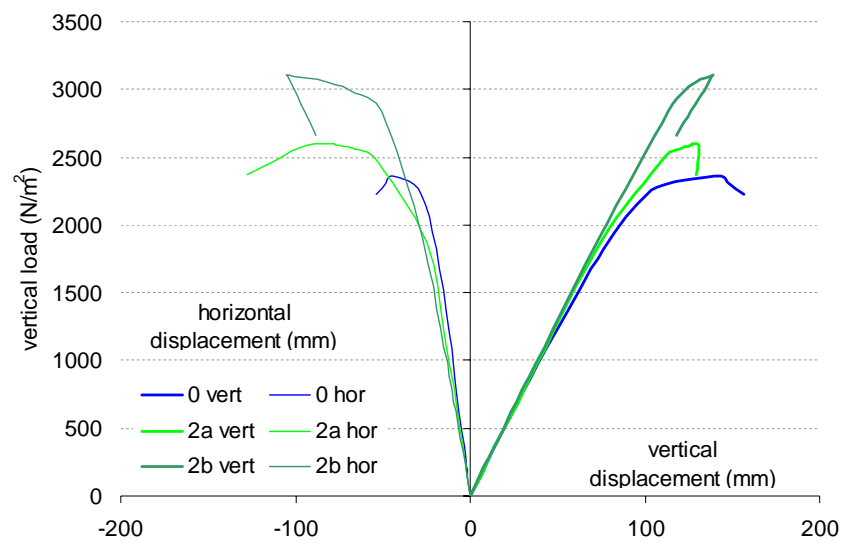


Figure 18 Load-displacement relationship (horizontal left, vertical right) of the restrained (Case 2) and unrestrained (Case 0) frames

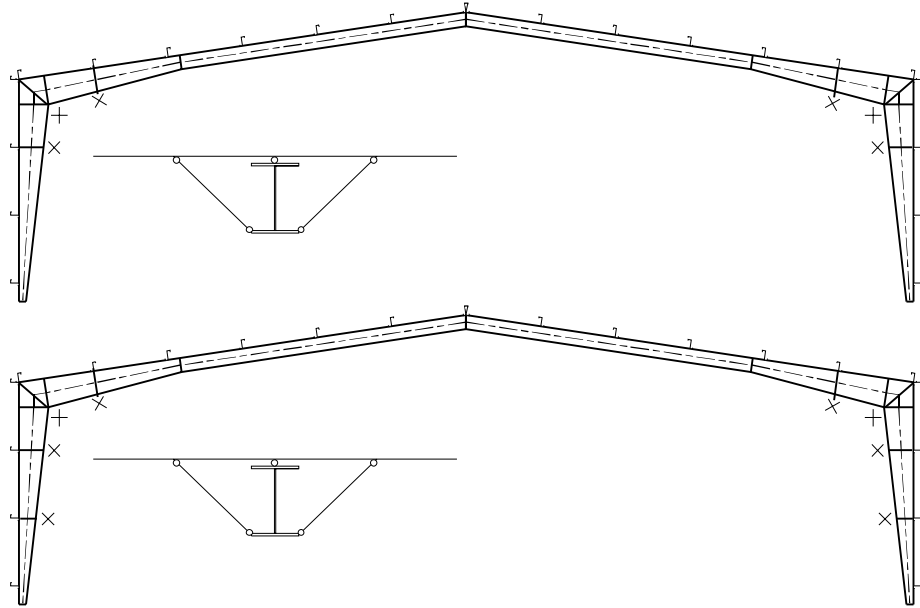


Figure 19 Case 3 with two purlins supports a) with one column support 4,2 m above the ground b) with two column supports starting from 2,3 m above the ground

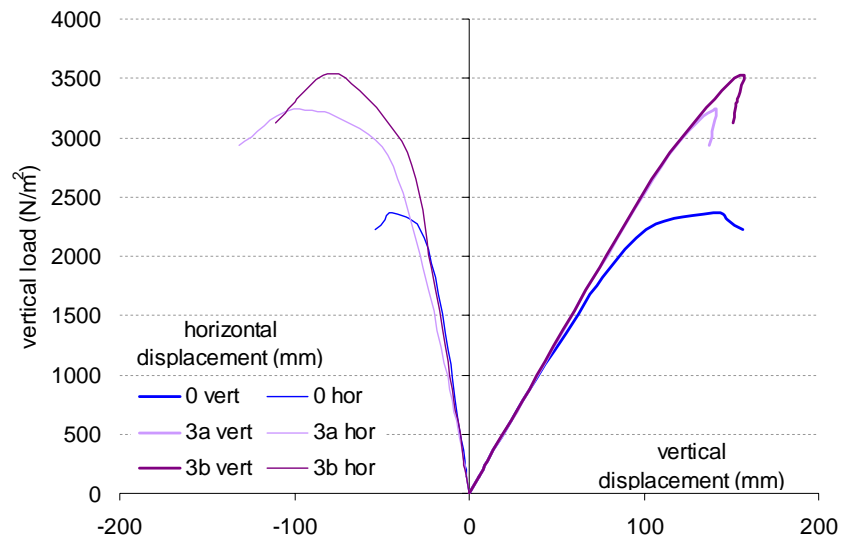


Figure 20 Load-displacement relationship (horizontal left, vertical right) of the restrained (Case 3) and unrestrained (Case 0) frames

The study clearly shows that the most efficient solutions are those with lateral supports concentrated around the frame corner (Case 3 and Case 4). Such frames were also used in optimization (Chapter 6.2).

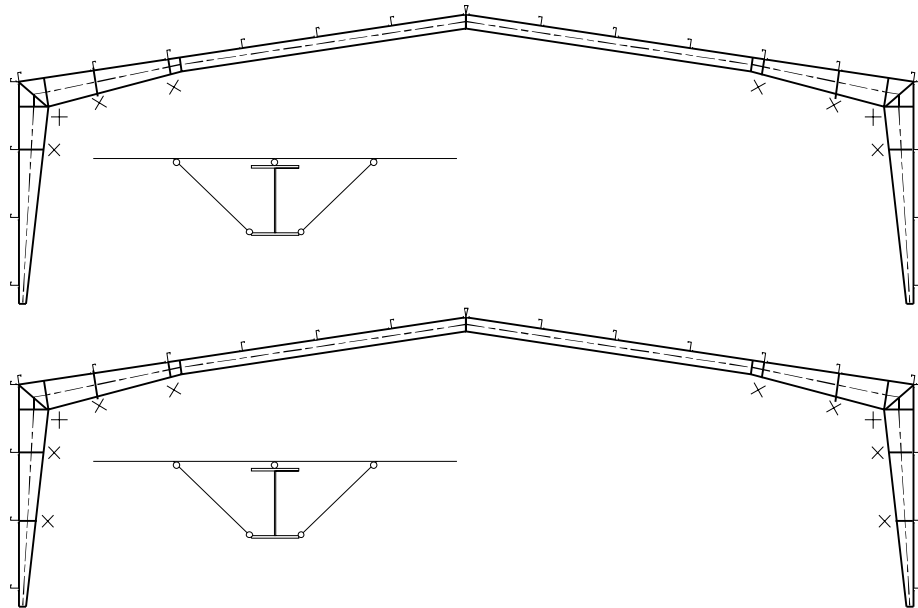


Figure 21 Case 4 with three purlins supports a) with one column support 4,2 m above the ground b) with two column supports starting from 2,3 m above the ground

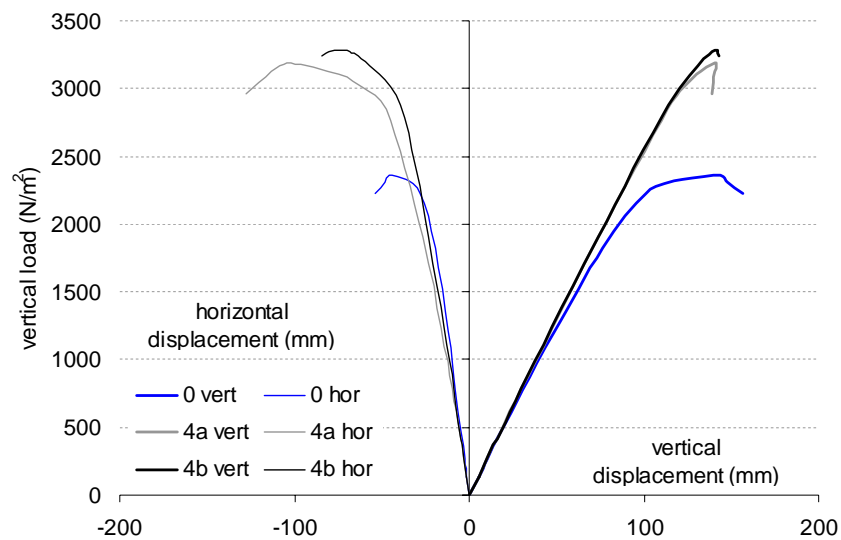


Figure 22 Load-displacement relationship (horizontal left, vertical right) of the restrained (Case 4) and unrestrained (Case 0) frames

7 Validation of results

In order to calibrate the tools, the results of the optimization study by Horridge et al. [18] have been replicated. A couple of important points in this study must be taken into consideration in order to understand the extent of calibration presented here:

- a) The configurations considered were based on the Universal Beam (UB) range of class 1 profiles allowing for plastic analysis. In line with British practice, first order plastic analysis was used for the design (i.e. no imperfections, no second order effects and no buckling were considered).
- b) The frames were considered pinned. Therefore the structures cannot develop a plastic mechanism with several plastic hinges.
- c) The eaves height was increasing together with the span and it should be noted that the steel consumption (Figure 23) was considerably affected by this fact.
- d) No serviceability checks were reported in the original study [18].
- e) The results are not based on any formal optimisation method, rather it was attempted to find optimal configurations based on engineering experience. The roof angle and the haunch length were fixed in advance.

The cases reported by Horridge et al. were reproduced using the EV-frame and AP-Frame tools. It was impossible to fully recover all original design assumptions because some incompatibilities exist between the old British codes and the Eurocode methods. Therefore, a few equivalent assumptions had to be used.

Namely:

- a) The AP-Frame and EV-Frame tools were forced to neglect lateral torsional buckling. This was achieved by setting buckling reduction factors to 1, and all out-of-plane imperfections to 0.
- b) The safety factors of loading were modified to match those used by Horridge et al. [18], i.e. $\gamma = 1.7$ for all loads.
- c) The basic wind speed of 46 m/s (3 seconds average) reported to be used with the British code, was replaced with 15.5 m/s (10 minutes average) wind speed compatible with EN 1991 [19] and producing the same total horizontal load. It should be noted that the factors controlling the wind pressure on the roof are also different in the two codes, but this difference has not been eliminated.
- d) The steel grade 43 reported by Horridge et al. [18] has been replaced by S275, with the same yield stress.
- e) Instead of the classic plastic method, allowing of the successive forming of plastic hinges, the calculation uses linear and nonlinear elastic analysis with plastic sectional properties, as described by EN 1993 [1]. This method could be adopted because frames are pinned and they cannot create successive plastic hinges.

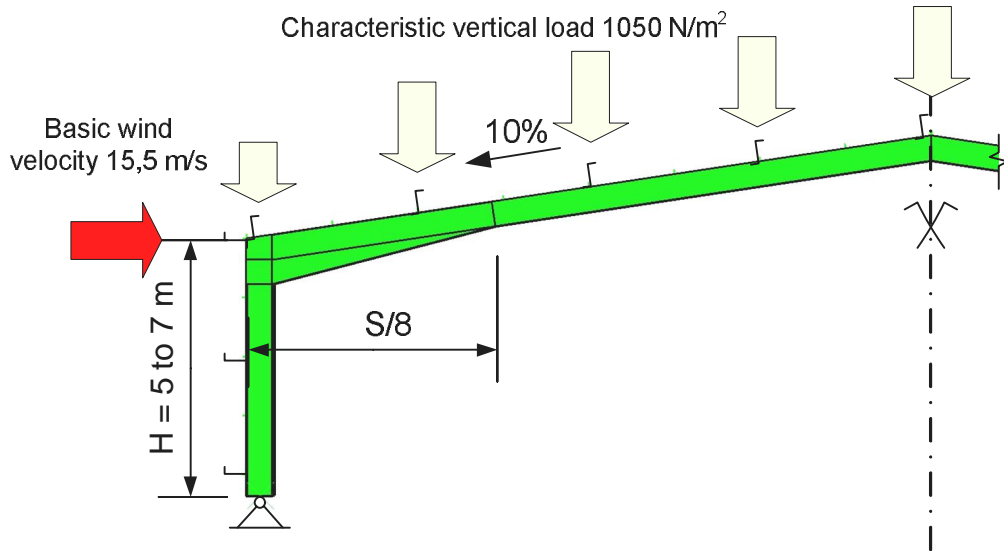


Figure 23 Geometry and loading of hot-rolled frames

The optimisation used by Horridge et al. [18] was emulated with the above assumptions, and the original configurations were re-calculated using EV-Frame and AP-Frame tools. These configurations had a ULS utilization factor in the range of 0.93-1.22 with EV-Frame and 0.88-1.13 with AP-Frame (Figure 24). It can be concluded that both software tools were able to recreate the initial set with good accuracy. EV-Frame is slightly more conservative, predicting an average utilization factor of 1.06, suggesting that the frame proposed by Horridge et al. [18] would fail using linear elastic analysis with plastic sectional properties. AP-Frame is less conservative with nonlinear elastic analysis based on equivalent plastic strain check to identify the plastic hinge. The average utilization factor was 0.98 and the method predicted problems with only few of original configurations.

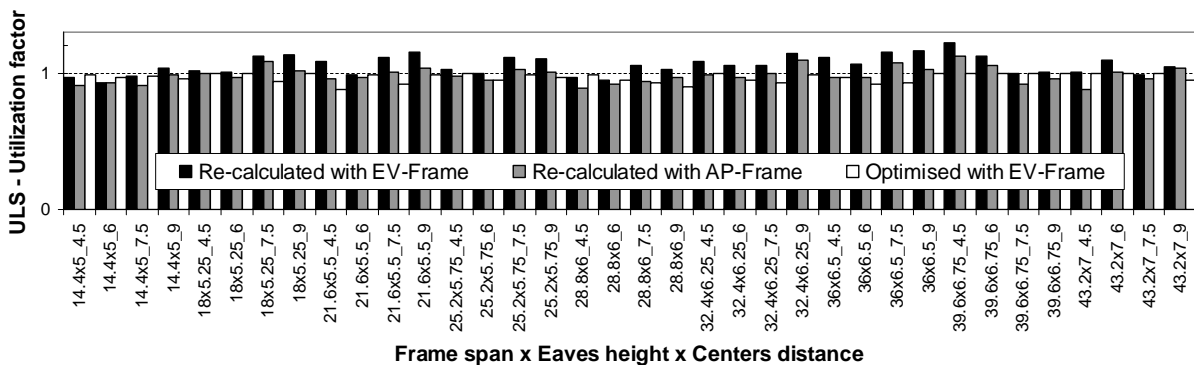


Figure 24 Recalculated and optimized cases utilization of ULS checks

The set of frame configurations used by Horridge et al. [18] have been optimized using the EV-Frame, with exactly the same constraints (Figure 25). While the original optimisation proved to be very good, we found that marginal improvements are possible even in this very rigorously studied set of frames.

For instance, the EV-Frame optimized frames had a slightly different balance between beam and column compared to the original frames. On average, plastic modulus of beams increased by 10% while plastic modulus of columns decreased

by 7%, suggesting that weaker beams and strongest columns, compared to the usage of Horridge et al. [18], are the optimal configuration.

In Figure 23, the steel consumptions are given for the frame distance 6 m, also considered in the original study. These consumptions were calculated using a single frame mass without any additional steel elements e.g. bracings, purlins, longitudinal beams etc. It can be observed that the original configurations by Horridge et al. [18] and the optimized ones by EV-Frame and AP-Frame have very similar weight.

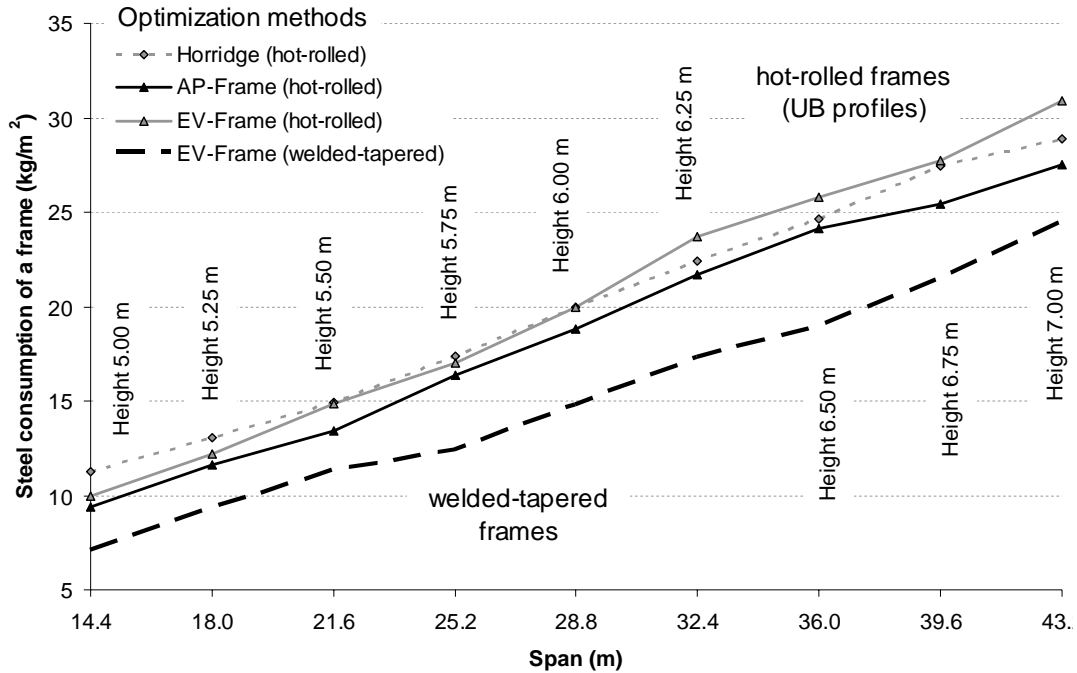


Figure 25 Comparison of different design and optimisation methods

Table 5 Optimization of hot-rolled frames by Horridge et al.

(a) Optimization of 5 to 7 m high frames with 4.5 m distances calculated by Horridge et al. with full lateral support					
Span (m)	Column	Rafter	Eaves height (m)	Frame mass (tons)	Steel consumption (kg/m ²)
14.4	UB305x127x37	UB254x102x25	5.00	0.787	12.1
18.0	UB356x171x51	UB254x146x31	5.25	1.184	14.6
21.6	UB457x191x67	UB305x127x37	5.50	1.671	17.2
25.2	UB533x210x82	UB356x171x45	5.75	2.257	19.9
28.8	UB533x210x92	UB406x178x54	6.00	2.895	22.3
32.4	UB610x229x101	UB406x178x60	6.25	3.513	24.1
36.0	UB686x254x125	UB457x191x67	6.50	4.413	27.2
39.6	UB762x267x147	UB457x191x74	6.75	5.388	30.2
43.2	UB762x267x147	UB533x210x92	7.00	6.620	34.1
(b) Optimization of 5 to 7 m high frames with 6 m distances calculated by Horridge et al. with full lateral support					
14.4	UB356x171x45	UB254x146x31	5.00	0.972	11.3
18.0	UB406x178x60	UB305x127x37	5.25	1.407	13.0
21.6	UB457x191x74	UB356x171x45	5.50	1.936	14.9
25.2	UB533x210x92	UB406x178x54	5.75	2.629	17.4
28.8	UB610x229x101	UB457x191x67	6.00	3.445	19.9
32.4	UB686x254x125	UB457x191x74	6.25	4.350	22.4
36.0	UB762x267x147	UB533x210x82	6.50	5.327	24.7
39.6	UB762x267x173	UB533x210x92	6.75	6.521	27.4
43.2	UB838x292x176	UB610x229x101	7.00	7.495	28.9
(c) Optimization of 5 to 7 m high frames with 7.5 m distances calculated by Horridge et al. with full lateral support					
14.4	UB356x171x51	UB305x127x37	5.00	1.132	10.5
18.0	UB457x191x74	UB305x165x40	5.25	1.623	12.0
21.6	UB533x210x92	UB356x171x51	5.50	2.288	14.1
25.2	UB610x229x101	UB406x178x60	5.75	2.924	15.5
28.8	UB686x254x125	UB457x191x74	6.00	3.985	18.5
32.4	UB686x254x140	UB533x210x82	6.25	4.820	19.8
36.0	UB762x267x173	UB533x210x92	6.50	6.062	22.5
39.6	UB838x292x176	UB610x229x113	6.75	7.542	25.4
43.2	UB914x305x201	UB686x254x125	7.00	9.008	27.8
(d) Optimization of 5 to 7 m high frames with 9 m distances calculated by Horridge et al. with full lateral support					
14.4	UB406x178x54	UB305x165x40	5.00	1.217	9.4
18.0	UB533x210x82	UB356x171x45	5.25	1.809	11.2
21.6	UB533x210x101	UB406x178x54	5.50	2.466	12.7
25.2	UB610x229x113	UB457x191x67	5.75	3.256	14.4
28.8	UB686x254x140	UB533x210x82	6.00	4.415	17.0
32.4	UB762x267x173	UB533x210x92	6.25	5.602	19.2
36.0	UB838x292x194	UB610x229x101	6.50	6.730	20.8
39.6	UB914x305x201	UB686x254x125	6.75	8.401	23.6
43.2	UB914x305x224	UB686x254x140	7.00	10.087	25.9

Table 6 Optimization of hot-rolled frames using EV-Frame tool

(a) Optimization of 5 to 7 m high frames with 4.5 m distances calculated with EV-Frame (Method 3) with full lateral support					
Span (m)	Column	Rafter	Eaves height (m)	Frame mass (tons)	Steel consumption (kg/m ²)
14.4	UB305x127x37	UB254x102x22	5.00	0.787	12.1
18.0	UB406x140x46	UB305x102x28	5.25	1.184	14.6
21.6	UB457x152x60	UB406x140x39	5.50	1.671	17.2
25.2	UB457x152x74	UB356x171x45	5.75	2.257	19.9
28.8	UB533x210x82	UB457x152x52	6.00	2.895	22.3
32.4	UB533x210x109	UB457x152x60	6.25	3.513	24.1
36.0	UB610x229x125	UB457x191x74	6.50	4.413	27.2
39.6	UB686x254x125	UB533x210x82	6.75	5.388	30.2
43.2	UB686x254x152	UB533x210x92	7.00	6.620	34.1
(b) Optimization of 5 to 7 m high frames with 6 m distances calculated with EV-Frame (Method 3) with full lateral support					
14.4	UB406x140x39	UB305x102x28	5.00	0.972	11.3
18.0	UB406x178x60	UB356x127x33	5.25	1.407	13.0
21.6	UB457x152x74	UB356x171x45	5.50	1.936	14.9
25.2	UB533x210x92	UB457x152x52	5.75	2.629	17.4
28.8	UB610x229x101	UB457x191x67	6.00	3.445	19.9
32.4	UB610x229x125	UB457x191x82	6.25	4.350	22.4
36.0	UB762x267x134	UB533x210x92	6.50	5.327	24.7
39.6	UB762x267x147	UB610x229x101	6.75	6.521	27.4
43.2	UB762x267x173	UB610x229x113	7.00	7.495	28.9
(c) Optimization of 5 to 7 m high frames with 7.5 m distances calculated with EV-Frame (Method 3) with full lateral support					
14.4	UB406x140x46	UB356x127x33	5.00	1.132	10.5
18.0	UB457x152x67	UB406x140x39	5.25	1.623	12.0
21.6	UB533x210x82	UB457x152x52	5.50	2.288	14.1
25.2	UB533x210x101	UB457x191x67	5.75	2.924	15.5
28.8	UB610x229x125	UB457x191x82	6.00	3.985	18.5
32.4	UB762x267x134	UB533x210x92	6.25	4.820	19.8
36.0	UB686x254x170	UB610x229x101	6.50	6.062	22.5
39.6	UB838x292x176	UB610x229x113	6.75	7.542	25.4
43.2	UB838x292x194	UB686x254x125	7.00	9.008	27.8
(d) Optimization of 5 to 7 m high frames with 9 m distances calculated with EV-Frame (Method 3) with full lateral support					
14.4	UB457x152x52	UB406x140x39	5.00	1.217	9.4
18.0	UB457x191x74	UB406x140x46	5.25	1.809	11.2
21.6	UB533x210x92	UB457x152x60	5.50	2.466	12.7
25.2	UB610x229x113	UB457x191x74	5.75	3.256	14.4
28.8	UB762x267x134	UB533x210x92	6.00	4.415	17.0
32.4	UB762x267x147	UB610x229x101	6.25	5.602	19.2
36.0	UB762x267x197	UB610x229x113	6.50	6.730	20.8
39.6	UB838x292x194	UB686x254x125	6.75	8.401	23.6
43.2	UB914x305x224	UB762x267x147	7.00	10.087	25.9

8 Conclusions

The advanced 3D modelling methods explored in this report are very effective, and offer the designer the ability to model complex structural configurations and support conditions. Because the simplified methods described in the design codes for special configurations are naturally conservative, the use of advanced options can bring substantial economical benefits.

On the other hand, due to advances in computing capabilities (both software and hardware), the use of these 3D shell models is not any more out of reach of an average design office. The calculation time in the range of a few minutes with the AP-frame tool is still long compared to the runtime in range of few seconds with beam-based analysis software, but both of them are much shorter compared to the time spent on creating the model. If the model preparation is automated (like in case of AP-Frame) the advanced tool is very competitive for single analysis.

In terms of optimization, the use of EV-Frame offers instant solution. It is clear that similar tools should be, and for some cases are, used by the design offices. The GA offers a strong and versatile option for optimization in the field of structural engineering.

The optimization time of advanced modelling AP-Frame tool is still in the range of many hours when used on a standard computer. However, the combination of 3D modelling and GAs can take the advantage of parallel computing and is especially suitable for server applications.

Concerning the specific results presented in this report, it has been shown that using slender welded-tapered frames instead of hot-rolled sections leads to decreased steel consumption. Cost savings could be achieved by implementing modern fabrication technologies. However, slender frames have to be properly designed especially considering their lateral stability. In order to effectively design the lateral restraints, calculation of 3D model is needed. The usual diagonal stay configuration of lateral restraint, when it relies on light-gauge steel purlins, is not effective in preventing the lateral buckling of the frame, especially in larger span frames. Further, implementing shape optimization into the design process provides economical solution tailored to the specific loading situation.

9 Summary

The results of the study clearly point to the advantages of using advanced modelling, e.g. GMNIA, instead of the classical member checks. While both methods are accepted by the current steel design code EN 1993, using GMNIA results in important savings, because it eliminates some of the conservativeness brought in by the unavoidable simplifications of the other methods. The experience shows that using complex 3D models is possible with current computational capabilities.

References

- [1] Hradil P., Mielonen M., Fülöp L., VTT R 00524 10 Research report, *Optimization tools for steel portal frames – software documentation*, Espoo, 2009
- [2] EN 1993:2005, Eurocode 3: Design of steel structures
- [3] Dowling P.J., Mears T., Owens G., Raven K., A development in the automated design and fabrication of portal framed industrial buildings, *The Structural Engineer*, vol. 60A, Oct. 1982, pp. 311-319.
- [4] Lee G.C., Ketter R.L., and HSU T., *The design of single storey rigid frames*, Cleveland, Ohio: Metal Building Manufacturers Association, 1981.
- [5] *Practical analysis of single-storey portal frames*, European Convention for Constructional Steelwork, 1991.
- [6] King C. M.. *Plastic design of single-storey pitched-roof portal frames to Eurocode 3*. Technical report. P147. UK: The Steel Construction Institute; 1995.
- [7] Salter P., Malik A., King C., *Design of Single-Span Steel Portal Frames to BS 5950-1:2000*, Great Britain: The Steel Construction Institute, 2004.
- [8] King, C. M., *SCI P164 Technical Report: Design of steel portal frames for Europe*, The Steel Construction Institute, 2001
- [9] Dowling P.J., Mears T., Owens G., Raven K., Discussion on: A development in the automated design and fabrication of portal framed industrial buildings, *The Structural Engineer*, vol. 61A, Dec. 1983, pp. 383-392.
- [10] EN 1998-1:2004, Eurocode 8: Design of structures for earthquake resistance
- [11] Davies J. M., Inplane stability in portal frames, *The Structural Engineer*, Volume 68, No. 8, April 1990.
- [12] Šapalas, V., Samofalov, M., Viačeslavas, Š FEM stability analysis of tapered beam-columns, *Journal of Civil Engineering and Management*, 2005, Volume XI., No. 3, 211-216.
- [13] Deb, K. & Gulati, S, Design of truss-structures for minimum weight using genetic algorithms, *Finite Elements in Analysis and Design*, 2001, vol. 37, no. 5, pp. 447-465.
- [14] Jalkanen, J. *Tubular truss optimisation using heuristic algorithms*, 2007, Tampere University of Technology.
- [15] Saka, M.P., Optimum design of pitched roof steel frames with haunched rafters by genetic algorithm, *Computers & Structures*, 2003, vol. 81, no. 18-19, pp. 1967-1978.
- [16] Mielonen, M-P. *Steel portal frame optimization using genetic algorithms*, 2010, Aalto University School of Science and Technology
- [17] Deb, K. & Agrawal, R.B., "Simulated binary crossover for continuous search space, *Complex Systems*, 1995, no. 9, pp. 115-148.
- [18] Horridge, J.F., Morris, L.J., Comparative costs of single-storey framed structures, *The Structural Engineer*, Vol. 64A, No. 7, July 1986
- [19] EN 1991, Eurocode 1: Actions on structures